Journal of Air Pollution and Health (Spring 2026); 11(2): 217-230

Original Article

Available online at http://japh.tums.ac.ir

Comparison of three functional regression methods on air pollution throughout the first two COVID-19 lockdown phases across 31 Iranian provinces

Mohammad Fayaz

Department of Public Health and Social Medicine, School of Medicine, Shahed University, Tehran, Iran

ARTICLE INFORMATION

Article Chronology:
Received 10 November 2025
Revised 02 March 2026
Accepted 06 June 2026
Published 29 June 2026

Keywords:
Air pollution; COVID-19 restrictions; Functional principal component analysis (FPCA); Function on function (FOF) regression; Meteorological covariates; Iran

CORRESPONDING AUTHOR:
m.fayaz@shahed.ac.ir
Tel: (+98 21) 55228800
Fax: (+98 21) 55228800

ABSTRACT

Introduction: Exposure to air pollution heightens respiratory vulnerability, particularly during pandemics. The COVID-19 lockdowns in Iran provided a natural experiment to investigate how reduced human activity influenced air quality across 31 provinces. Understanding these environmental responses is vital for informing sustainable public health and pollution mitigation policies.

Materials and methods: Satellite derived data on air pollutants and air quality and meteorological variables were obtained for all 31 provinces of Iran from Sentinel-5P, the GLDAS 2 dataset developed by National Aeronautics and Space Administration (NASA), and Google Earth Engine (GEE). The study covered two COVID-19 lockdown periods and their corresponding pre pandemic periods from the previous year. The evaluated air quality indices consisted of Carbon monoxide (CO), Water Vapor (H_2O,) Nitrogen dioxide (NO_2), Ozone (O_3), Sulfur dioxide (SO_2), Absorbing Aerosol Index (AER), and Atmospheric Formaldehyde (HCHO). Meteorological covariates comprised temperature, pressure, precipitation, and wind speed. Sparse temporal data were reconstructed using FDA and FPCA, representing Functional Data Analysis and Functional Principal Component Analysis, respectively. Three Function on Function (FOF) regression models standard, smooth, and principal component based were developed, with and without meteorological adjustments. Model performance was assessed using R^2, AIC, and BIC, representing the coefficient of determination, Akaike Information Criterion, and Bayesian Information Criterion, respectively.

Results: Air pollutant levels significantly declined during both lockdowns compared with the corresponding pre pandemic periods, with spatial variations influenced by meteorological and industrial factors. Incorporating meteorological covariates markedly improved model accuracy, particularly for NO_2 and CO. The principal component based FOF model provided the best fit, explaining over 80% of variance in major pollutants.

Conclusion: COVID-19 lockdowns produced measurable, regionally heterogeneous improvements in air quality across Iran. Integrating meteorological adjustments and advanced functional regression approaches enhances environmental modeling and supports evidence based air pollution control strategies during health emergencies.

Please cite this article as: Fayaz M. Comparison of three functional regression methods on air pollution throughout the first two COVID-19 lockdown phases across 31 Iranian provinces. Journal of Air Pollution and Health. 2026;11(2): 217-230.
Doi: https://doi.org/10.18502/japh.v11i2.21879

Introduction

Exposure to atmospheric pollutants over both brief and prolonged periods has been associated with adverse COVID-19 outcomes. In particular, fine particulate matter measuring ≤2.5 μm in aerodynamic diameter ($PM_{2.5}$) has been linked to higher COVID-19 transmission and mortality in the United States [1, 2], China [3-5], Italy [6], Spain, France, and Germany [7], as well as across Asia [8] and other countries worldwide [9]. Moreover, air pollution has been identified as an important confounding variable in studies examining racial disparities in COVID-19 cases and fatalities within the United States [10]. In addition to pollution-related factors, meteorological conditions—especially elevated temperatures—have also been reported to substantially affect global COVID-19 transmission patterns [11].

Although air pollution and meteorological conditions are recognized as important factors in COVID-19-related research, many investigations have primarily focused on the effects of pandemic restrictions on transportation and industrial operations. These restrictions provided a distinctive setting for environmental policymakers to evaluate existing assumptions and develop alternative approaches for controlling global pollution levels. In India, substantial reductions in air pollutant concentrations were reported during lockdown periods [12], prompting suggestions for periodic two- or four-day restrictions as a potential strategy for air pollution mitigation while accounting for economic consequences and seasonal fluctuations [13]. The economic impacts associated with air pollution during the COVID-19 pandemic have been investigated, highlighting the importance of implementing more rigorous environmental regulations [14]. Nevertheless, these preventive measures failed to substantially decrease severe air pollution in certain regions of China because of prevailing meteorological and atmospheric chemical conditions [15]. Despite this, lockdown measures positively influenced global public perceptions of air quality improvement [16, 17].

In this regard, new technologies are now able to measure various atmospheric conditions. For instance, air pollution monitoring using the AURA satellite of the Earth Observation System (EOS), operated by the National Aeronautics and Space Administration (NASA), in China has shown a reduction in CO (Carbon Monoxide) and NO_2 (Nitrogen Dioxide) levels over the COVID-19 pandemic period, attributed to transportation restrictions and reduced economic activities [18]. Satellite measurements from MODIS (Moderate-resolution Imaging Spectroradiometer) show declining $PM_{2.5}$ concentrations across various nations [19]. Research further indicates a global decline in air pollution based on analyses from Google Earth Engine (GEE) and Apple mobility datasets [20]. This decrease is statistically significant across multiple air pollution indicators in Iran and neighboring countries [21].

This study investigates the impact of COVID-19 restrictions on air pollution indices across Iran and its provinces during two restriction waves, using two datasets obtained from GEE (Google Earth Engine) , including satellite-derived observations: 1) Air Quality and Air Pollution indices (Sentinel-5P) and 2) Meteorological indices (GLDAS-2). We also applied novel and advanced statistical methodologies such as FDA (functional data analysis) and FOF regression (function-on-function) and considering the weather condtion variables in

two regresstion strategies to investiage their effects.The FDA models consider the time series as whole curves and used dimension redctuion methods like Functional Principal Components Analysis (FPCA) and smoothing methods such as B-Spline.

Materials and methods

The methods are briefly outlined in the following subsections.

Data collection procedures and management

Administrative boundary shapefiles for Iran's 31 provinces were downloaded from ArcGIS Online. Two sets of indices were used: (1) air quality and pollution variables derived from the Sentinel-5P Near Real-Time (NRTI) satellite product, including CO (Carbon Monoxide), H_2O (Water Vapor), NO_2 (Nitrogen Dioxide), O_3 (Ozone), SO_2 (Sulfur Dioxide), AER (Absorbing Aerosol Index), and HCHO (Atmospheric Formaldehyde), and (2) meteorological variables from GLDAS-2 (Global Land Data Assimilation System Version 2), developed by NASA (National Aeronautics and Space Administration), including pressure, total precipitation rate, air temperature, and wind speed. These data were retrieved from GEE (Google Earth Engine) Data Catalog.

COVID-19 restrictions included limitations on transportation, government operations, and educational institutions such as schools and universities, as well as increased reliance on online activities (21). In this study, two comparative periods were considered: (1) the 37-day first wave lockdown period (March 14–April 20, 2020) compared with the corresponding period in 2019 (March 14–April 20, 2019), and (2) the 12-day second wave lockdown period (April 13–April 25, 2021) compared with the equivalent period in 2020 (April 13–April 25, 2020) in Iran.

Functional data analysis (FDA)

The air quality and pollution indices ,X_{ijwC} (t), and meteorological indices, M_{kjwC} (t), are treated as functional data with the following index sets{X_{ijwC} (t),i=1,…,7 ,j=1,…,31,w=1,2 ,C=1,2} and {M_{kjwC} (t),k=1,…,4 ,j=1,… ,31,w=1,2 ,C=1,2}. Here, i represents the name of the air quality and pollution indices, k represents the name of the meteorological indices, j denotes the province, w represents the COVID-19 wave (first and second), and C indicates the COVID-19 status (previous year and pandemic year) [22]. The X_{ijwC} (t) data include missing values and are considered sparse functional data. Consequently, the FPCA (functional principal component analysis) method for sparse data is applied using the FPCA() function from the fdapace library. Each X_{ijwC} (t) is centered and scaled, then decomposed into eigenfunctions and eigen scores, with a percentage of variance Explained (PVE)≥0.99. Subsequently, each X_{ijwC} (t) is reconstructed based on the FPCAs. Two modeling strategies are then applied, including function-on-function regression (FOF) using the pffr() function from the refund library for each X_{ijwC} (t) : [23-25].

$$Startegy\ I:\ X_{ijw2}(t) = f_0(t) + \int_S X_{ijw1}(s)\beta_{1,iw}(t,s)ds + \epsilon_i(t)$$
$$\epsilon_i(u) \sim N(0, \sigma_\epsilon^2) \quad (1)$$

$$Startegy\ II:\ X_{ijw2}(t) = f_0(t) + \int_S X_{ijw1}(s)\beta_{1,iw}(t,s)\,ds + \int_S M_{1jw2}(s)\beta_{2,iw}(t,s)\,ds + \int_S M_{2jw2}(s)\beta_{3,iw}(t,s)\,ds + \int_S M_{3jw2}(s)\beta_{4,iw}(t,s)\,ds + \int_S M_{4jw2}(s)\beta_{5,iw}(t,s)\,ds$$

$$\epsilon_i(u) \sim N(0, \sigma_\epsilon^2) \quad (2)$$

In Model (1), the air quality and pollution indices during the COVID-19 period, X_{jw2} (t), t ϵ T or days during COVID-19 restriction, are only associated with the previous year's indices, X_{ijw1} (s), s ϵ S or same days during previous year without any COVID-19 restriction, through the estimated coefficient $\beta_{1,iw}$ (t,s). However, in model (2), the air quality and pollution indices during COVID-19 period, X_{ijw2} (t), are related to the previous year's indices, X_{ijw1} (s), with the estimated coefficient $\beta_{1,iw}$ (t,s), and are additionally adjusted by four metrological variables M_{1jw2} (s), M_{2jw2} (s), M_{3jw2} (s) and M_{4jw2} (s), with estimated coefficients $\beta_{2,iw}$ (t,s), $\beta_{3,iw}$ (t,s), $\beta_{4,iw}$ (t,s) and $\beta_{5,iw}$ (t,s), respectively.

To estimate the model parameters, three FOF regression methods were employed: function-on-function regression [ff()], smooth function-on-function regression [sff()], and principal component-based function-on-function regression [ffpc()]. The results were compared and validated using R^2 (Coefficient of Determination), AIC (Akaike's Information Criterion), and BIC (Bayesian Information Criterion). The best-performing model among the three FOF estimation approaches was selected based on higher R^2 values and lower AIC and BIC criteria.. The estimated coefficients are plotted as heatmap with pointwise p-values as black lined regions overlayed ($\alpha<0.05$ is considered as statistical significant).

Results and discussion

Descriptive satistics

The calculated changes in estimated mean values and percentage increases for each atmospheric contamination indicator are reported together with statistical significance analyses using both distribution-based and distribution-free methods, by contrasting the pandemic restriction period against the same dates in the preceding year. These results are presented separately for the first and second waves, grouped by province [26].

Effective degrees of freedom and model fit quality

As shown in Table 1, the estimated Effective Degrees of Freedom (EDF) and their corresponding p-values are compared between models I and II for each wave and air pollution index. EDF exceeding 2 suggest a strong non-linear association between the dependent variable and the explanatory factors [27]. The p-values for most covariates are statistically significant at $\alpha=0.05$. For example, the NO_2 in the first wave and both model I (unadjusted) and model II (adjusted) have the edf for previuse year of the NO_2 equal to 5.33 and 7.96 , respectively and they have p-values less than 0.05 which means the relationship are highly non-linear and statistically significant. In the second wave, the same relationship have edf equal to 5.06 and 5.56 respectively and the p-values are less than 0.05.

Table 1. Estimated EDF and corresponding P-values FOF regression models, grouped by air pollution indices, lockdown waves, and model strategies in Iran

Air Quality Indices	Waves	Model Strategy	Covariates			
			Previous Year of COVID-19	Pressure	Precipitation	Temperature
CO	1	I	1 (<0.05)	-	-	-
		II	1 (<0.05)	1 (<0.05)	1 (0.42)	1 (0.26)
	2	I	1 (<0.05)	-	-	-
		II	1 (0.05)	1 (<0.05)	1.03 (0.25)	1 (0.05)
H_2O	1	I	1.97 (<0.05)	-	-	-
		II	9.46 (<0.05)	4.07 (<0.05)	1 (0.56)	3.13 (<0.05)
	2	I	5.11 (<0.05)	-	-	-
		II	5.08 (<0.05)	2.95 (<0.05)	8.69 (<0.05)	1 (<0.05)
NO_2	1	I	5.33 (<0.05)	-	-	-
		II	7.96 (<0.05)	1 (0.92)	10.14 (<0.05)	2.04 (0.1)
	2	I	5.06 (<0.05)	-	-	-
		II	5.56 (<0.05)	1.06 (0.14)	2.56 (0.33)	4.5 (<0.05)
O_3	1	I	9.89 (<0.05)	-	-	-
		II	3.55 (<0.05)	1 (<0.05)	2.09 (0.05)	4.41 (<0.05)
	2	I	1 (<0.05)	-	-	-
		II	4.14 (<0.05)	1.37 (0.17)	1.45 (0.67)	3.51 (<0.05)

Table 1. Continued

Air Quality Indices	Waves	Model Strategy	Covariates				
			Previous Year of COVID-19	Pressure	Precipitation	Temperature	Wind
SO_2	1	I	1.65 (0.28)	-	-	-	-
		II	1 (0.26)	1 (0.89)	1 (0.56)	1.6 (0.45)	1 (0.91)
	2	I	4.88 (<0.05)	-	-	-	-
		II	2.04 (<0.05)	1 (0.42)	1.85 (0.28)	2.03 (<0.05)	3.02 (<0.05)
AEI	1	I	1 (<0.05)	-	-	-	-
		II	2.47 (<0.05)	1 (0.26)	10.2 (<0.05)	1 (0.66)	1 (0.17)
	2	I	2.69 (<0.05)	-	-	-	-
		II	1.91 (0.2)	1 (<0.05)	2.85 (0.53)	1 (<0.05)	5.68 (<0.05)
HCHO	1	I	1 (<0.05)	-	-	-	-
		II	1 (<0.05)	1 (0.26)	1 (0.31)	1 (0.1)	2.44 (0.41)
	2	I	9 (<0.05)	-	-	-	-
		II	10.63 (<0.05)	3.16 (<0.05)	1 (0.14)	1.55 (0.33)	1.71 (0.08)

*- *Estimated EDF (P-Value)*

Each cell presents the estimated EDF followed by its significance level (P-value) in parentheses. Model I represents the unadjusted model, and Model II includes meteorological covariates (pressure, precipitation, temperature, and wind).

Comparison of FOF regression models

Table 2 presents a comparison of the goodness-of-fit statistics for the three FOF regression methods used in strategy II across three models for both waves, grouped by air pollution index names. The NO_2 models for both wave 1 and wave 2 exhibit the highest R^2 values with ffpc(), achieving 80.01% and 89.53%, respectively. Overall, the models for wave 2 show higher R^2 values than those for wave 1. In most cases, the ffpc() method produces the highest or nearly the highest R^2 values. In addition, the lowest AIC and BIC are bold and they indicate the best model based on these goodness of fit indices.

Table 2. Model fit evaluation measures for the three FOFregression approaches (ff, sff, and ffpc), categorized according to atmospheric pollutant indicators and lockdown phases in Iran

Air Quality Indices	Models	Wave 1			Wave 2		
		R-Sqr	AIC	BIC	R-Sqr	AIC	BIC
CO	ff	51.05%	4815.23	4850.57	61.06%	1432.37	1460.01
	sff	51.86%	4822.41	4979.18	66.28%	1411.32	1560.36
	ffpc	51.25%	4842.76	5034.81	65.33%	1427.61	1596.80
H_2O	ff	34.26%	11306.57	11424.15	46.22%	3465.84	3580.93
	sff	34.95%	11315.57	11531.42	51.10%	3455.57	3662.39
	ffpc	34.73%	11332.68	11617.92	51.14%	3458.87	3681.98
NO_2	ff	76.91%	8429.37	8587.71	84.52%	2856.79	2933.67
	sff	78.06%	8399.58	8687.21	85.00%	2865.87	3022.18
	ffpc	80.01%	8297.40	8644.58	89.53%	2743.76	2966.85
O_3	ff	51.60%	2590.99	2673.81	21.69%	797.82	856.81
	sff	51.85%	2592.68	2718.70	24.40%	803.68	935.56
	ffpc	52.25%	2600.59	2810.55	24.16%	802.76	932.35
SO_2	ff	2.45%	14981.95	15062.70	28.63%	3125.25	3177.36
	sff	2.01%	15001.09	15158.40	33.68%	3125.86	3279.71
	ffpc	5.70%	14975.12	15226.48	49.08%	3047.46	3292.76
AEI	ff	18.49%	6604.98	6706.22	20.08%	2134.56	2201.84
	sff	19.34%	6614.37	6818.56	26.69%	2125.65	2279.90
	ffpc	17.55%	6654.60	6929.84	55.39%	1967.63	2242.44
HCHO	ff	9.40%	11629.68	11674.23	39.16%	3440.64	3532.16
	sff	11.56%	11628.41	11793.54	40.43%	3452.29	3617.46
	ffpc	11.87%	11633.22	11846.44	48.96%	3415.76	3662.32

- The bold numbers are the highest R^2 and lowest AIC and BIC in each gas.
- The table presents the R^2 (coefficient of determination), AIC (Akaike Information Criterion), and BIC (Bayesian Information Criterion) for each model during the first and second COVID-19 lockdown waves. Larger R^2 values together with smaller AIC and BIC scores reflect superior model accuracy and overall fit.

Estimated coefficients and P-Values

Fig. 1 and Fig. 2 illustrate the estimated coefficient surfaces obtained using ff() for the atmospheric quality indicators during the first and second waves, respectively. The colors represent the range of estimated coefficient values, from low (dark blue) to high (red). Pointwise p-values are overlaid on each graph with a contour map, highlighting statistically significant regions. In figure 1, the horizontal axis represents days 1–36 from the corresponding period of the preceding year, whereas the vertical axis denotes days 1–36 during the initial COVID-19 wave. In figure 2, the x-axis corresponds to days 1–12 from the equivalent period in the previous year, while the y-axis represents days 1–12 during the second wave of COVID-19.

The patterns of the estimated betas differ. For instance, in Fig. 1, H_2O shows three positive values, resembling isolated regions in yellow to red, with statistical significance at $\alpha < 0.01$. The coefficients for CO, NO_2, O_3, AEI, and HCHO coefficients are all positive and most of them are statistically significant at $\alpha < 0.01$.

In Fig. 1 each surface is adjusted for four climatic covariates (pressure, precipitation, temperature, and wind), with corresponding p-values represented by contour lines.

A comparison between Fig. 1 and Fig. 2 shows that their patterns differ between the first and second waves of the COVID-19 lockdowns. However, the patterns for CO and AEI are nearly identical across both waves.

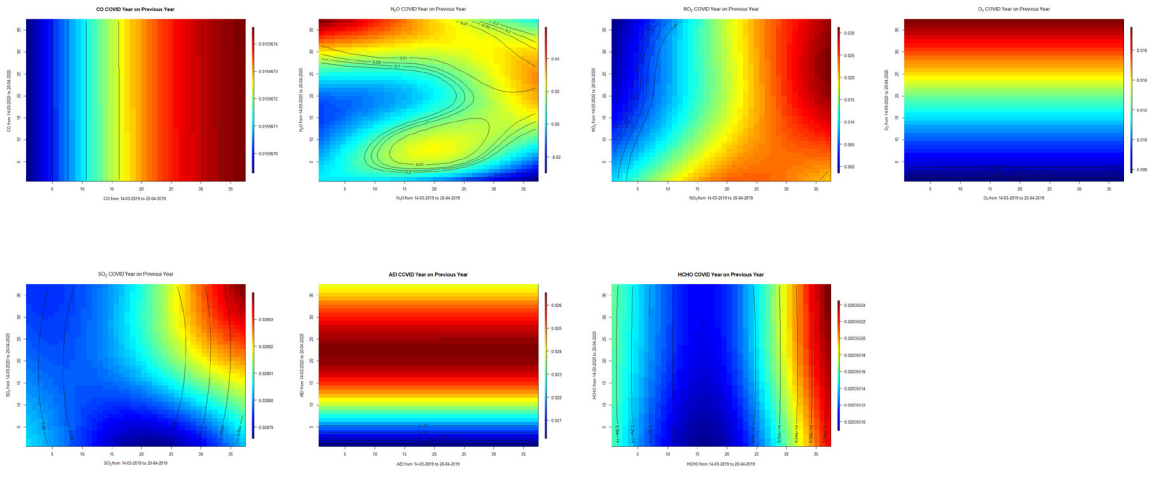

Fig. 1. Estimated coefficient surfaces for seven distinct FOF regression models based on the ff() approach across different air pollution indices during the first COVID-19 lockdown wave in Iran

In Fig. 2 each surface is adjusted for four climatic covariates (pressure, precipitation, temperature, and wind), with corresponding p-values represented by contour lines.

Spatial pattern showing the differences between observed measurements and model-predicted estimates

Maps illustrating the mean differences between observed and predicted values, derived from the FOF regression using ffpc() for each air pollution index and lockdown wave, are presented separately. For instance, the maps for NO_2 are shown in Fig. 3. In both plots A and B, the colors range are near zero with grey color, indicating that the predicted and observed values for all provinces are very similar. However, Tehran and Alborz provinces are shaded in blue or dark blue, indicating that the observed values are higher than the predicted values in plot A. Provinces near Tehran, such as Qom, Markazi, Qazvin, Gilan, Mazandaran, and Golestan, are also shown in purple in wave 1. Maps for other air quality indices can be found in [26].

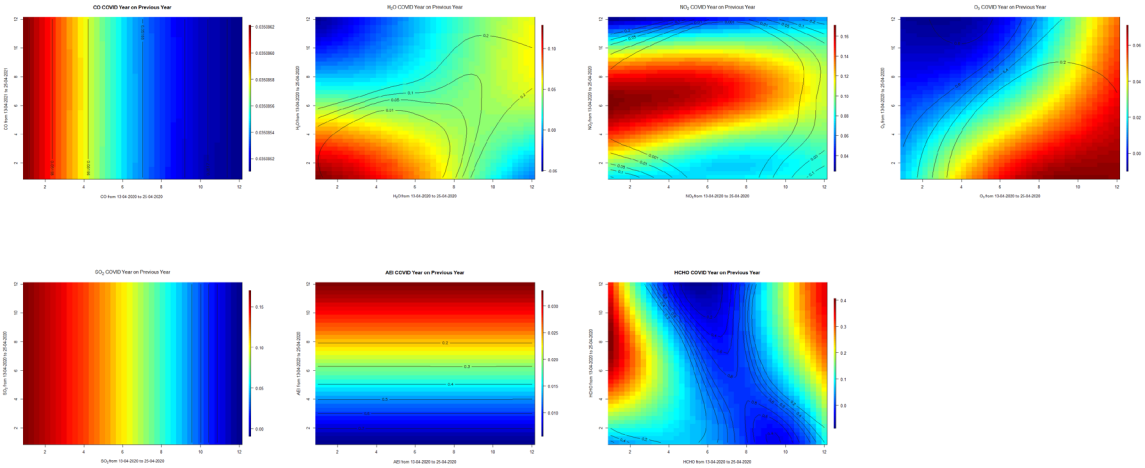

Fig. 2. Estimated coefficient surfaces for seven distinct FOF regression models based on the ff() approach across different air pollution indices during the second COVID-19 lockdown wave in Iran

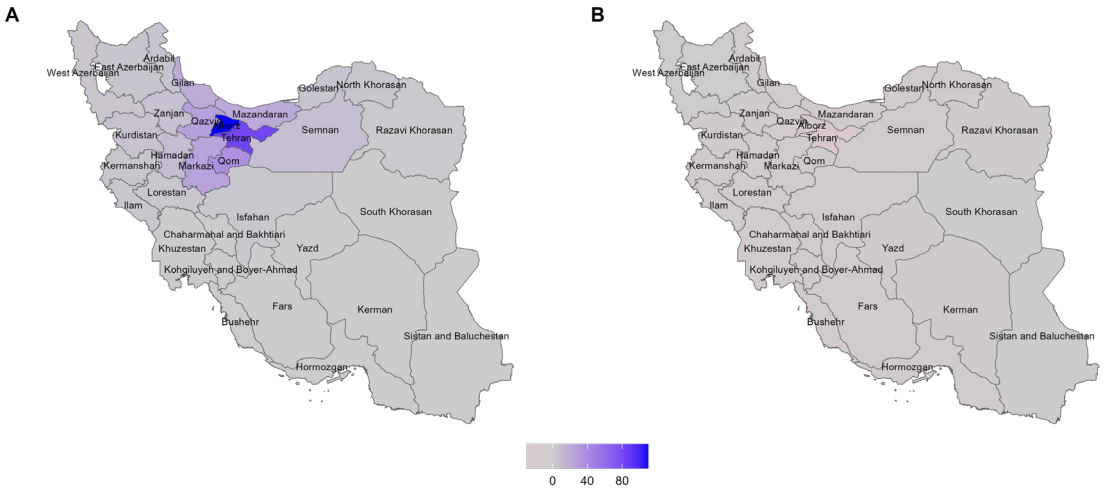

Fig. 3. Differences between observed and predicted values obtained from the ffpc-based Functional-On-Functional regression (pffr()) model for NO_2 (×1,000,000) during the COVID-19 lockdowns in Iran

In Fig. 3 Panel (A) represents the first wave, and Panel (B) represents the second wave.

Several studies have documented decreases in air pollution levels across Iranian provinces during the COVID-19 lockdown period. For example, a decrease in $PM_{2.5}$ was observed from February 19, 2020, to March 11, 2020, across all provinces [28], , while other studies reported reductions in $PM_{2.5}$, PM_{10}, and NO_2 across 12 cities in Iran [29]. Further research using GEE methods found declines in NO_2 and CO in Iran and four cities [30]. Additional findings showed decreases in CO, NO_2, $PM_{2.5}$, and PM_{10}, along with increases in SO_2 and O_3 during the first wave, as well as a reduction in the Air Quality Index (AQI) across four provinces equipped with 150 monitoring stations [31]. Similar patterns were also reported for CO, NO_2, and O_3 in Isfahan [32, 33], Arak province [34], and Tehran [35-38], while reductions in Aerosol Optical Depth (AOD) were observed in Khuzestan province [39]. Moreover, decreases in $PM_{2.5}$, NO_2, and O_3 in Khorramabad, were reported in Khorramabad, the capital of Lorestan province [40, 41] , and in Bojnurd city in North Khorasan [42]. While our study reached most of the prevouse results, it also estimates the relationships and dynamic changes in days and spatial variations.

On the other hand, the Containment and Health Index (C&H) is a composite indicator that integrates the Stringency Index with additional variables from the Oxford Coronavirus Government Response Tracker (OxCGRT) project. It is scaled from 0 to 100 and represents the strictness of governmental COVID-19 response policies, including measures such as mobility restrictions, mask requirements, and other related interventions. During Iran's first COVID-19 lockdown period (March 14 to April 20, 2020), the C&H index had an average value of 37.09 with a standard deviation of 3.128. In contrast, during the second wave (April 13–25, 2021), the C&H index showed a mean of 71.916 with a standard deviation of 0.572. We conclude that air quality improved more during the first wave, whereas the C&H index reached higher levels in the second wave [43].

Only a limited number of studies have investigated air pollution across both COVID-19 waves. For example, the decrease in NO_2 levels during the first wave was more pronounced than that observed in the second wave worldwide [44]. In Spain, NO_2 was found to be the most influential variable among meteorological indicators associated with COVID-19 incidence and severity across both waves [45, 46]. In contrast, NO_2 concentrations were higher during the second COVID-19 wave compared with the first lockdown period in India [47]. On the other hand, in Australia, NO_2 reductions were more substantial during the second wave than in the first, likely due to more stringent restrictions [48]. Our study compares both waves and examines how their patterns change over time on a daily basis.

Recent studies on climatic indices in Iran that applied fuzzy clustering methods [49] did not utilize any Functional Data Analysis (FDA) techniques; therefore, extending fuzzy clustering approaches with FDA-based methods represents a promising direction for future research. Another recent work [21] , along with the present study, is among the first to integrate the GEE dataset with Functional Data Analysis (FDA) methods, highlighting a promising avenue for future research. Lastly, an important limitation of this study is the lack of data from air quality monitoring stations operated by Iran's Department of Environment..

Conclusion

This study demonstrates the substantial effects of COVID-19 lockdowns on air pollution levels across 31 provinces of Iran,

utilizing satellite-based data to monitor environmental changes during periods of public health restrictions. By applying FPCA and comparing three FOF regression models, we demonstrate that advanced statistical methods can effectively reconstruct sparse data and model complex temporal patterns. Incorporating meteorological covariates, such as temperature and wind, markedly improved model performance, underscoring the role of environmental factors in air quality assessment [26]. The differential effects observed between the first and second lockdowns reveal notable regional variability, providing critical insights for policymakers to design targeted air quality management strategies during public health crises.

Financial supports

No funding was received for conducting this study.

Competing interests

The author declares that they have no known competing financial interests or personal relationships that could have appeared to influence the work reported in this paper.

Acknowledgements

Author acknowledges the Research Square for hosting our preparation.

Ethical considerations

Ethical issues (Including plagiarism, Informed Consent, misconduct, data fabrication and/or falsification, double publication and/or submission, redundancy, etc) have beencompletely observed by the authors.

References

1. Wu X, Nethery RC, Sabath MB, Braun D, Dominici F. Exposure to air pollution and COVID-19 mortality in the United States: A nationwide cross-sectional study. MedRxiv. 2020.

2. Wu X, Nethery RC, Sabath MB, Braun D, Dominici F. Air pollution and COVID-19 mortality in the United States: Strengths and limitations of an ecological regression analysis. Science advances. 2020;6(45):eabd4049.

3. Xie J, Zhu Y. Association between ambient temperature and COVID-19 infection in 122 cities from China. Science of the Total Environment. 2020;724:138201.

4. Zhu Y, Xie J, Huang F, Cao L. Association between short-term exposure to air pollution and COVID-19 infection: Evidence from China. Science of the total environment. 2020;727:138704.

5. Ma Y, Zhao Y, Liu J, He X, Wang B, Fu S, et al. Effects of temperature variation and humidity on the death of COVID-19 in Wuhan, China. Science of the total environment. 2020;724:138226.

6. Conticini E, Frediani B, Caro D. Can atmospheric pollution be considered a co-factor in extremely high level of SARS-CoV-2 lethality in Northern Italy? Environmental pollution. 2020;261:114465.

7. Ogen Y. Assessing nitrogen dioxide (NO_2) levels as a contributing factor to coronavirus (COVID-19) fatality. Science of the Total Environment. 2020;726:138605.

8. Baniasad M, Mofrad MG, Bahmanabadi B, Jamshidi S. COVID-19 in Asia: Transmission factors, re-opening policies, and vaccination simulation. Environmental research. 2021;202:111657.

9. Pansini R, Fornacca D. Early spread of

COVID-19 in the air-polluted regions of eight severely affected countries. Atmosphere. 2021;12(6):795.

10. Millett GA, Jones AT, Benkeser D, Baral S, Mercer L, Beyrer C, et al. Assessing differential impacts of COVID-19 on black communities. Annals of epidemiology. 2020;47:37-44.

11. Scafetta N. Distribution of the SARS-CoV-2 pandemic and its monthly forecast based on seasonal climate patterns. International journal of environmental research and public health. 2020;17(10):3493.

12. Shehzad K, Sarfraz M, Shah SGM. The impact of COVID-19 as a necessary evil on air pollution in India during the lockdown. Environmental Pollution. 2020;266:115080.

13. Mahato S, Pal S, Ghosh KG. Effect of lockdown amid COVID-19 pandemic on air quality of the megacity Delhi, India. Science of the total environment. 2020;730:139086.

14. Bashir MF, Ma B, Shahzad L. A brief review of socio-economic and environmental impact of Covid-19. Air Quality, Atmosphere & Health. 2020;13(12):1403-9.

15. Wang P, Chen K, Zhu S, Wang P, Zhang H. Severe air pollution events not avoided by reduced anthropogenic activities during COVID-19 outbreak. Resources, Conservation and Recycling. 2020;158:104814.

16. Lou B, Barbieri DM, Passavanti M, Hui C, Gupta A, Hoff I, et al. Air pollution perception in ten countries during the COVID-19 pandemic. Ambio. 2022;51(3):531-45.

17. Barbieri DM, Lou B, Passavanti M, Hui C, Lessa DA, Maharaj B, et al. Survey data regarding perceived air quality in Australia, Brazil, China, Ghana, India, Iran, Italy, Norway, South Africa, United States before and during Covid-19 restrictions. Data in brief. 2020;32:106169.

18. Filonchyk M, Hurynovich V, Yan H, Gusev A, Shpilevskaya N. Impact assessment of COVID-19 on variations of SO_2, NO_2, CO and AOD over East China. Aerosol and air quality research. 2020;20(7):1530-40.

19. Bherwani H, Kumar S, Musugu K, Nair M, Gautam S, Gupta A, et al. Assessment and valuation of health impacts of fine particulate matter during COVID-19 lockdown: a comprehensive study of tropical and sub tropical countries. Environmental Science and Pollution Research. 2021;28(32):44522-37.

20. Venter ZS, Aunan K, Chowdhury S, Lelieveld J. COVID-19 lockdowns cause global air pollution declines. Proceedings of the National Academy of Sciences. 2020;117(32):18984-90.

21. Fayaz M. The lock-down effects of COVID-19 on the air pollution indices in Iran and its neighbors. Modeling earth systems and environment. 2022:1-7.

22. Ramsay JO, Silverman B, . Functional Data Analysis: Springer New York, NY; 2005. XIX, 429 p.

23. Xiao L, Li C, Checkley W, Crainiceanu C. Fast covariance estimation for sparse functional data. Statistics and computing. 2018;28:511-22.

24. Crainiceanu CM, Goldsmith J, Leroux A, Cui E. Functional data analysis with R: CRC Press; 2024.

25. Fayaz M, Abadi A, Khodakarim S. The Functional Regression With Reconstructed Functions From Hybrid Principal Components Analysis: With EEG-fMRI Application. Statistics, Optimization & Information Computing. 2022;10(3):890-903.

26. Fayaz M. mohammad-fayaz GitHub profile 2026 [Available from: https://github.com/mohammad-fayaz.

27. Hunsicker ME, Kappel CV, Selkoe KA, Halpern BS, Scarborough C, Mease L, et al. Characterizing driver–response relationships

in marine pelagic ecosystems for improved ocean management. Ecological applications. 2016;26(3):651-63.

28. Asna-ashary M, Farzanegan MR, Feizi M, Sadati SM. COVID-19 outbreak and air pollution in Iran: a panel VAR analysis. MAGKS Joint Discussion Paper Series in Economics; 2020.

29. Norouzi N, Asadi Z. Air pollution impact on the Covid-19 mortality in Iran considering the comorbidity (obesity, diabetes, and hypertension) correlations. Environmental Research. 2022;204:112020.

30. Shami S, Ranjgar B, Bian J, Khoshlahjeh Azar M, Moghimi A, Amani M, et al. Trends of CO and NO_2 Pollutants in Iran during COVID-19 Pandemic Using Timeseries Sentinel-5 Images in Google Earth Engine. Pollutants. 2022;2(2):156-71.

31. Rad AK, Shariati M, Zarei M. The impact of COVID-19 on air pollution in Iran in the first and second waves with emphasis on the city of Tehran. Journal of Air Pollution and Health. 2020;5(3):181-92.

32. Moazeni M, Maracy MR, Dehdashti B, Ebrahimi A. Spatiotemporal analysis of COVID-19, air pollution, climate, and meteorological conditions in a metropolitan region of Iran. Environmental Science and Pollution Research. 2022;29(17):24911-24.

33. Roshan G, Sarli R, Fitchett JM. Urban heat island and thermal comfort of Esfahan City (Iran) during COVID-19 lockdown. Journal of Cleaner Production. 2022;352:131498.

34. Karimi B, Moradzadeh R, Samadi S. Air pollution and COVID-19 mortality and hospitalization: An ecological study in Iran. Atmospheric Pollution Research. 2022:101463.

35. Keshtkar M, Heidari H, Moazzeni N, Azadi H. Analysis of changes in air pollution quality and impact of COVID-19 on environmental health in Iran: application of interpolation models and spatial autocorrelation. Environmental Science and Pollution Research. 2022;29(25):38505-26.

36. Namdar-Khojasteh D, Yeghaneh B, Maher A, Namdar-Khojasteh F, Tu J. Assessment of the relationship between exposure to air pollutants and COVID-19 pandemic in Tehran city, Iran. Atmospheric Pollution Research. 2022;13(7):101474.

37. Khorsandi B, Farzad K, Tahriri H, Maknoon R. Association between short-term exposure to air pollution and COVID-19 hospital admission/ mortality during warm seasons. Environmental Monitoring and Assessment. 2021;193(7):1-6.

38. Hashemi F, Hoepner L, Hamidinejad FS, Abbasi A, Afrashteh S, Hoseini M. A survey on the correlation between PM2. 5 concentration and the incidence of suspected and positive cases of COVID-19 referred to medical centers: A case study of Tehran. Chemosphere. 2022;301:134650.

39. Broomandi P, Crape B, Jahanbakhshi A, Janatian N, Nikfal A, Tamjidi M, et al. Assessment of the association between dust storms and COVID-19 infection rate in southwest Iran. Environmental Science and Pollution Research. 2022;29(24):36392-411.

40. Anbari K, Sicard P, Omidi Khaniabadi Y, Raja Naqvi H, Rashidi R. Assessing the effect of COVID-19 pandemic on air quality change and human health outcomes in a capital city, southwestern Iran. International Journal of Environmental Health Research. 2022:1-12.

41. Rashidi R, Khaniabadi YO, Sicard P, De Marco A, Anbari K. Ambient PM2. 5 and O_3 pollution and health impacts in Iranian megacity. Stochastic Environmental Research and Risk Assessment. 2022:1-10.

42. Aboubakri O, Ballester J, Shoraka HR, Karamoozian A, Golchini E. Ambient temperature and Covid-19 transmission: An evidence from a region of Iran based on weather station

and satellite data. Environmental Research. 2022;209:112887.

43. Ritchie H, Mathieu E, Rodés-Guirao L, Appel C, Giattino C, Ortiz-Ospina E, et al. Coronavirus pandemic (COVID-19). Our world in data. 2020.

44. Wang H, Tan J, Li X. Global NO 2 dynamics During the COVID-19 pandemic: a comparison between two waves of the coronavirus. IEEE Journal of Selected Topics in Applied Earth Observations and Remote Sensing. 2021;14:4310-20.

45. Bañuelos Gimeno J, Blanco A, Díaz J, Linares C, López J, Navas M, et al. Air pollution and meteorological variables' effects on COVID-19 first and second waves in Spain. International Journal of Environmental Science and Technology. 2022:1-14.

46. Linares C, Culqui D, Belda F, López-Bueno JA, Luna Y, Sánchez-Martínez G, et al. Impact of environmental factors and Sahara dust intrusions on incidence and severity of COVID-19 disease in Spain. Effect in the first and second pandemic waves. Environmental Science and Pollution Research. 2021;28(37):51948-60.

47. Dutta A, Dutta G. Association of air pollution and meteorological variables with the two waves of COVID-19 pandemic in Delhi: A critical analysis. Heliyon. 2021;7(11):e08468.

48. Boroujeni M, Saberian M, Li J. Environmental impacts of COVID-19 on Victoria, Australia, witnessed two waves of Coronavirus. Environmental Science and Pollution Research. 2021;28(11):14182-91.

49. Aghelpour P, Singh VP, Varshavian V. Time series prediction of seasonal precipitation in Iran, using data-driven models: a comparison under different climatic conditions. Arabian Journal of Geosciences. 2021;14(7):1-14.